# Performance of a novel aeration microbubble generator in aquaculture

[1,2]Imam Taukhid, [3]Dody D.Trijuno, [3]Muhammad Y. Karim, [2]Rachman Syah, [2]Makmur

[1] PhD Student Fisheries Science, Faculty of Marine Science and Fisheries, Hasanuddin University, Makassar, Indonesia; [2] Ministry of Marine Affairs and Fisheries Research Institute for Coastal Aquaculture and Fisheries Extention, Maros, Indonesia; [3] Faculty of Marine Science and Fisheries, Hasanuddin University, Makassar, Indonesia. Corresponding author: I. Taukhid, taukhidi19l@student.unhas.ac.id

**Abstract**. In aquaculture, aeration through microbubble generators often experiences blockages due to the cross-section area and a small air hole diameter. Therefore, this study modifed the induction of pumps equipped with piping systems that function like nozzles. A novel method of experimental design was used to convert the submersible pumps into aeration microbubble generators, by enlarging the nozzle and air hole diameter. The tests were performed for nozzle and air hole diameters were 32.5 mm and 22.4 mm, respectively, at different airflow rates speeds, namely 0.5, 1.5 and 2.5 L min$^{-1}$. Based on the results, the maximum SOTE of 11% was produced at 2.5 L min$^{-1}$.

**Key Words**: airflow rate, aerator performance, microbubble generator, oxygen transfer efficiency.

**Introduction**. Aeration is the use of atmospheric or pure oxygen to increase the dissolved oxygen (DO) concentration in a column of water. It is important in high-density aquaculture because aeration is naturally insufficient (Jayanthi et al 2021; Marappan et al 2020). Meanwhile, growth and development in aquaculture require a DO concentration ranging from 4 to 7 mg L$^{-1}$ (Mukherjee & Chandrakant 2003), while concentrations ranging from 0.5 to 1.1 mg L$^{-1}$ induce stress and might lead to death (Allan & Maguire 1991; Boyd 1989). Therefore, an adequate aeration system is needed in high-density aquaculture (Jayanthi et al 2021; Tierney et al 2020; Zhang et al 2020).

There are various types of aeration systems in aquaculture, including a microbubble generator (MBG). This system produces micrometer-sized bubbles and speeds up the process of increasing DO concentrations (Budhijanto et al 2017; Heriyati et al 2020; Jeon et al 2018; Tsutsumi 2010). Furthermore, there are various types of MBG, namely: injectors (Budhijanto et al 2017; Tsutsumi 2010), spherical ball (Sadatomi et al 2005), orifice (Basso et al 2018; Juwana et al 2019; Sadatomi et al 2012), venturi (Huang et al 2019; Huang et al 2020; Itoh et al 2019; Majid et al 2018; Wang et al 2020; Wilson et al 2021), nozzle (Lee et al 2019; Masakazu et al 2011), direct air (Jeon et al 2018; Warjito et al 2016) and swirl flow (Alam et al 2018). However, the various types of MBG generally still have limitations when applied to aquaculture. For example, the addition of direct air ducts to the pump inlet leads to a constant discharge of water. Meanwhile, the addition of compressor aids for air demand tends to increase the need for electrical power and, in general, the cross-sectional area of nozzles, venturi and orifice, as well as the diameter of small air ducts. Thereby, the system easily gets blocked by dirt.

To address the limitations of the various MBG types, modifications were made, by enlarging the cross-sectional area of the nozzle and the diameter of the air duct mounted on the pump inlet, using a piping system equipment that is easy to assemble and to obtain from the market. Therefore, this study aimed to develop an MBG applicable for aeration in aquaculture. The tests were performed at a various airflow speed to determine the MBG performance.

***Principles and theoretical analysis of aeration***. The dissolved oxygen deficit was computed each time when the dissolved oxygen is measured during the reaeration (Boyd 1986, 1998). The equation is as follows:

$$\text{DO deficit}=C_s-C_m$$

Where:
$C_s$ - the dissolved oxygen concentration at saturation (mg $L^{-1}$);
$C_m$ - the measured dissolved oxygen concentration (mg $L^{-1}$).

Furthermore, the oxygen transfer coefficient was determined using the equation (Boyd 1986; Ruttanagosrigit et al 1991) described as follows:

$$K_La_T=\frac{\ln(\text{DO deficit}_{10})-\ln(\text{DO deficit}_{70})}{(t_{70}-t_{10})/60}$$

Where:
$K_La_T$ - oxygen transfer coefficient (hour$^{-1}$);
Ln - natural logarithm;
DO $\text{deficit}_{10}$ - DO deficit at 10% saturation (mg $L^{-1}$);
DO $\text{deficit}_{70}$ - DO deficit at 70% saturation (mg $L^{-1}$);
$t_{10}$ - time at 10% saturation (min);
$t_{70}$ - time at 70% saturation (min).

Hence, the coefficient of oxygen transfer at a temperature of 20℃ is calculated using the equation (ASCE 2007; Stenstrom & Gilbert 1981):

$$K_La_{20}=K_La_T/1.024^{T_{20}}$$

Where:
$K_La_{20}$ - oxygen transfer coefficient at 20°C;
1.024 - Theta factor.

The oxygen transfer rate is used to estimate the standard oxygen transfer value in the aerator using the equation (ASCE 2007; Boyd & Tucker 1998):

$$SOTR=(K_La_{20})(C_{s20})(V)\left(10^{-3}\right)$$

Where:
SOTR - the standard oxygen transfer rate (kg of oxygen hour$^{-1}$);
$C_{s20}$ is the concentration (mg $L^{-1}$) of dissolved oxygen at saturation and at 20°C, at a measurable salinity;
V - the volume of the tank ($m^3$);
$10^{-3}$ - conversion factor (kg into g).

Furthermore, SOTR is defined as the amount of oxygen transferred by the aerator into the water per hour.
The standard aeration efficiency (SAE) is the rate of oxygen transfer per unit power input (ASCE 2007). It is calculated as follows:

$$SAE=\frac{SOTR}{\text{Power Input}}$$

The oxygen transfer efficiency (OTE) refers to the fraction of oxygen, in an injected gas stream, dissolved under given conditions. Meanwhile, the standard oxygen transfer efficiency (SOTE) refers to the OTE at a given gas rate. The gas flow measurements for the oxygen transfer systems need to be accurately and precisely performed. The gas flow value is required to determine the OTE of the system and the potentially suitable test devices include orifice, venturi and pitot tubes used with appropriate traversing methods (ASCE 2007; Eckenfelder et al 2002; Herrmann-Heber et al 2020). The equation is as follows:

$$\text{SOTE} = \frac{\text{SOTR}}{W_{air}} \times 100$$

Where:
$W_{air}$ - mass flow rate (kg $s^{-1}$);
$W_{air}$ - (1.23 kg/$m^3$) Qs;
Qs - airflow speed ($m^3$ $s^{-1}$).

## Material and Method

***Description of the submersible pump***. The pump inlet was combined with a modified piping system, where the reducing socket serves as a nozzle with diameter 32.5 mm and the T reducer as an air hole with 22.4 mm, as seen in Figure 1 and Figure 2. Changes in the cross-sectional area of the reducing socket alter the pressure of the flow speed to attract free air through the T reducer. Therefore, there is a two-phase flow between water, air and the mixture by the impeller, producing a micrometer-sized bubble on the pump outlet. The submersible pump specification is as follows: model PG-12000, power 160 Watts, Qmax 12,000 L $hour^{-1}$, Hmax 4.5 m, inlet diameter 45 mm, outlet diameter 45 mm. The used airflow rate controller was a SHLLJ Shunhuanliu Liangyi Biao.

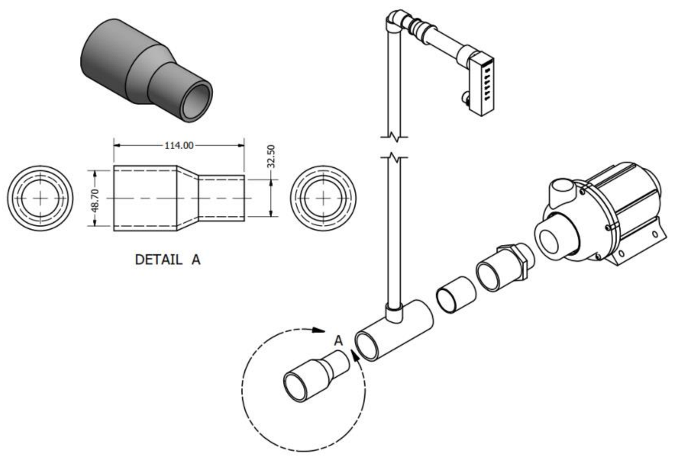


Figure 1. Installation of the microbubble generator device.

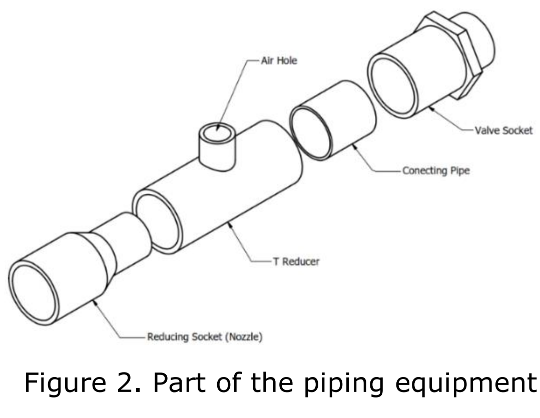


Figure 2. Part of the piping equipment.

***Experimental tank***. The test container used was a 1,100 L IBC tank cut off at the top, with the dimensions of 1.16 × 1.16 × 1.14 m, available at the Punaga Takalar Experimental Pond Installation, Research Center for Brackish Aquaculture Fisheries and Maros fishery extension. To avoid the weather influence on testing, the tank was equipped with a roof and an outlet valve at the lower side, for water disposal.

***Dissolved oxygen meter***. The dissolved oxygen meter (YSI Professional Pro Plus) was used to measure DO concentrations. Meanwhile, temperature and salinity were recorded along with DO with data transmission settings every 5 minutes. In addition, the DO meter was also connected to laptops with already installed YSI software application for easy observation.

***Chemicals used in the experiment***. To determine the performance of the MBG aeration, the DO in the test water needs to be eliminated until its concentration reaches 0.0 mg $L^{-1}$. Therefore, 20 mg $L^{-1}$ of sodium sulfite ($Na_2SO_3$) were used for the water deaeration through oxydation, together with 0.5 mg $L^{-1}$ of cobalt chloride ($CoCl_2$) as catalyst (Adel et al 2019; Ahmad 1987; ASCE 2007; Boyd & Ahmad 1987; Boyd & Tucker 1998,2014; Eckenfelder et al 2002). Thereafter, the water was stirred until the DO concentration reached 0.0 mg $L^{-1}$.

***Aeration experiments***. Aeration experiments were conducted in tanks of IBC 1,100 L using clean tap water. However, it can also be performed using seawater (Ruttanagosrigit et al 1991). Initially, the tap water was deoxygenated using sodium sulfite and cobalt chloride, as mentioned earlier. When the DO concentration reached 0.0 mg $L^{-1}$, the MBG was operated and simultaneous readings were taken periodically until DO increased from zero to almost 90% saturation. Furthermore, DO measurements were performed using two YSI Proplus meters and approximately 20 readings were taken every 5 minutes. Meanwhile, the DO deficit was calculated through the slope of the best fit line, which is the natural logarithm (Y) is plotted against time (X) (Boyd 1986,1998; Jayraj et al 2018).

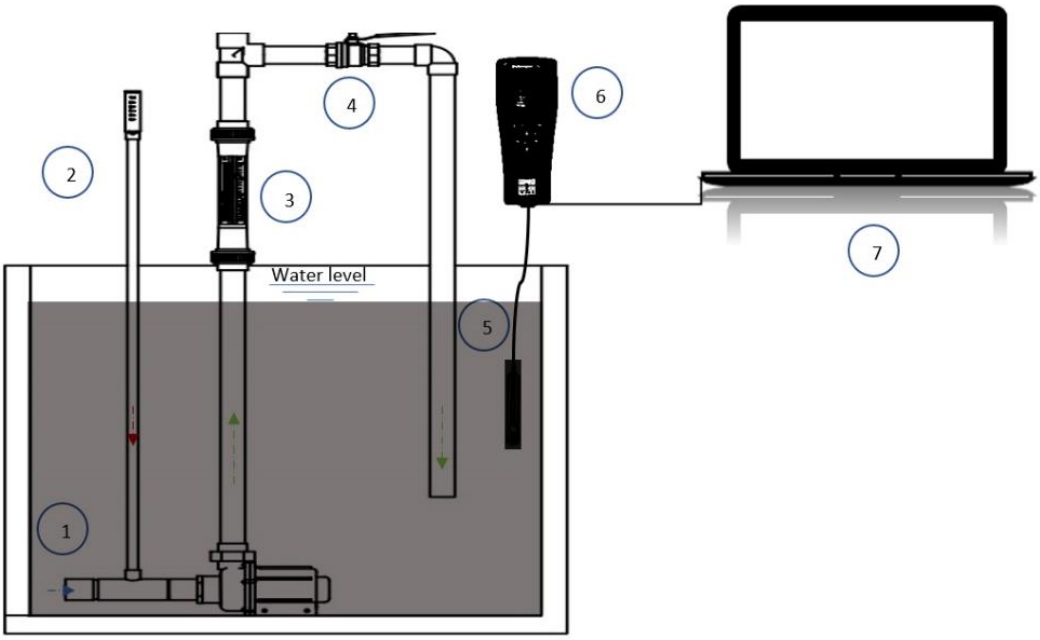


Figure 3. Diagram of the aeration microbubble generator system used in the experiments (1-water inlet; 2-rotometric airflow meter; 3-water flowmeter; 4-valve; 5-sensor; 6-YSi Proplus; 7-laptop).

**Results**. The first series of tests were conducted using a 32.5 mm nozzle with an air diameter of 22.4 mm, as shown in Figure 1 and Figure 2. Their results were used to determine the best combination of variables for further testing. Furthermore, the results showed that DO deficit and saturation oxygen increased linearly with respect to the airflow speed, as shown in Figure 4. The parameter performance of DIYM $O_2^{Rs}$ can be seen in Table 1.

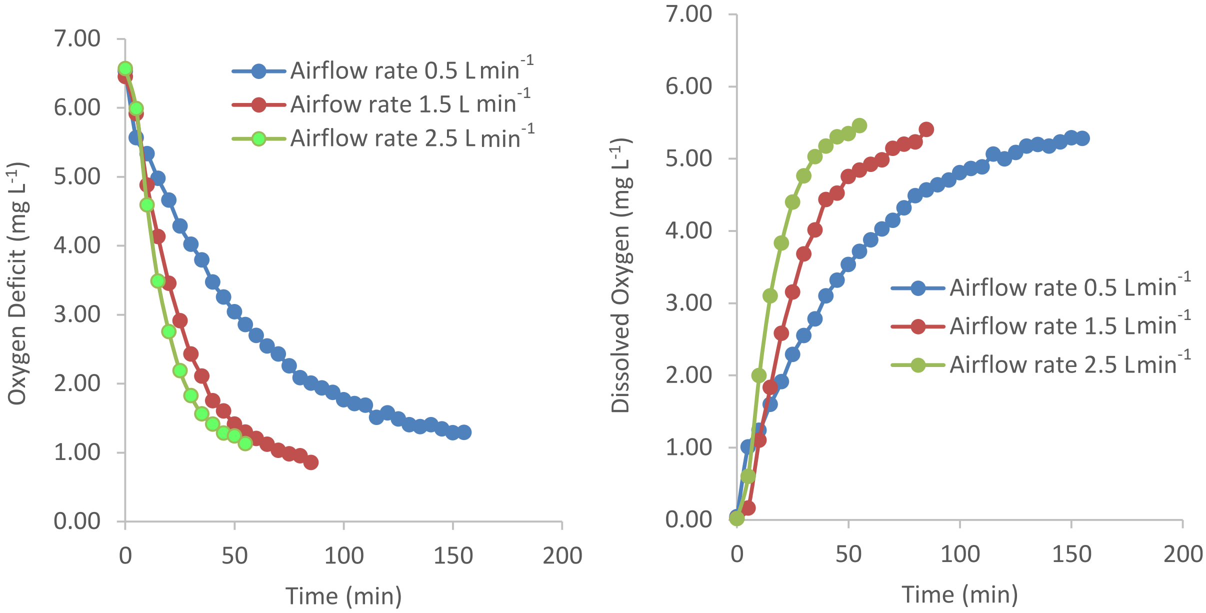


Figure 4. Effect of airflow rate, deficit and increased dissolved oxygen level.

Table 1

Performance of MBG at different airflow rate

| *Power (kW)* | *Diameter nozzle (mm)* | *Diameter air hole (mm)* | *Airflow rate (L min$^{-1}$)* | *$K_La_T$ (h)* | *$K_La_{20}$ (h)* | *SOTR (kg $O_2$ h$^{-1}$)* | *SAE (kg $O_2$ kWh$^{-1}$)* | *SOTE (%)* |
|---|---|---|---|---|---|---|---|---|
| | | | 0.5 | 0.84 | 0.70 | 0.006 | 0.04 | 15 |
| 0.16 | 32.5 | 22.4 | 1.5 | 1.99 | 1.68 | 0.014 | 0.08 | 12 |
| | | | 2.5 | 2.96 | 2.51 | 0.020 | 0.13 | 11 |

The slope of the linear line DO Deficit vs time (Figure 4) provides data to calculate the MBG. Meanwhile, Table 1 presents $K_La_T$, $K_La_{20}$, SOTR, SAE, and SOTE parameters of MBG performance at different airflow speeds. The results showed that the performance parameters were directly proportional to the airflow speeds, except the SOTE value. Moreover, at an airflow speed of 0.5 L min$^{-1}$, a minimum mass transfer coefficient of 0.84 was obtained. Meanwhile, at a maximum airflow speed of 2.5, a mass transfer coefficient of 2.96 was obtained. The SOTR and SAE values also increased with the airflow speed. Meanwhile, SOTE decreased along an increase in the airflow speed.

**Discussion**. DIYM $O_2^{RS}$ with nozzle serves to change the pressure in the nozzle by drawing free air through the T Reducer to control the airflow speed. Therefore, the airflow speed significantly affects the MBG system. When the system is mounted on the pump inlet, it produces a more acceptable diameter due to the bubbles rupture in the pump impeller (Cubas et al 2020). Higher airflow speeds lead to lower DO deficits and accelerate oxygen saturation time, as shown in Figure 4. This occured due to the increasing amount of air entering the MBG system, while the outlet accelerates the diffusion process to increase oxygen levels. Moreover, higher airflow levels affect the bubble surface area and size distribution (Abbas et al 2014; Jeon et al 2018).

The dissolved oxygen concentrations at different airflow rate levels represents saturated dissolved oxygen concentrations and DO deficits. Based on the results, the dissolved oxygen concentrations increased over time at varying airflow rates, while the oxygen concentration gradients decreased continuously. The increased diffusion rate of dissolved oxygen concentration decreases at the time of saturation. According to Fick's law, an increase in dissolved oxygen concentration in liquids leads to a decrease in the oxygen content per unit area and in the concentration gradient (Dai et al 2020). At an airflow rate speed of 2.5 L $min^{-1}$, the dissolved oxygen concentration in the aeration tank increased rapidly. Meanwhile, at 0.5 L $min^{-1}$, the increase in the oxygen concentration was slower. This is due to the oxygen concentration in the air. Hence, the higher the amount of air that enters, the faster the oxygen saturation process.

The $K_La_T$ volumetric oxygen mass transfer coefficient in Table 1 shows that the minimum yield at an airflow rate of 0.5 L $min^{-1}$ was 0.84. Meanwhile, at the highest airflow speed of 2.5 L $min^{-1}$, it was 2.96. Based on the results, the $KLa_T$ value increases with an rising airflow rate. This shows better results compared to the previous MBGs designed by Majid et al (2018), with $K_La_T$ values ranging from 0.015-0.05, and Sadatomi et al (2012) with lower $KLa_T$ value ranging from 0.005–0.013. Notwithstanding, the air speed in the aforementioned studies was higher (Majid et al 2018; Sadatomi et al 2012). Theoretically, higher air flow speeds induce higher turbulence in test containers (Majid et al 2018). In addition, turbulent flow also accelerate oxygen transfer during the test processes (Sadatomi et al 2005).

The SOTR Table 1 shows that the minimum yield at an airflow rate of 0.5 L $min^{-1}$ was 0.006 kg $O_2$ $h^{-1}$, meanwhile, the highest yield at 2.5 L $min^{-1}$ was 0.02 kg $O_2$ $h^{-1}$. Furthermore, the SOTR value obtained was lower compared to a previous study, which obtained 0.06 kg $O_2$ $h^{-1}$ at an airflow speed of 3.3 L $min^{-1}$, with a pump power of 400 watts (Zhang et al 2020). However, according to Abdelrahman & Veverica (2016), SOTR values for the MBG system range from 0.004–0.035 kg $O_2$ $h^{-1}$.

The airflow speed strongly influences the value of SOTE. The lower the air density, the higher the SOTE value. The higher the airflow speed, the lower the SOTE value. Based on the results, the maximum SOTE of 11% was produced at an airflow speed of 2.5 L $min^{-1}$. This result correlates with Abbas et al (2014). However, it requires a flow rate speed of 1.2 $m^3$ $h^{-1}$ or equivalent to 20 L $min^{-1}$.

**Conclusions**. In this study, a novel MBG DIYM $O_2^{RS}$ aeration device was constructed and its characteristics were examined. This new method utilizes the supply of free airflow through T reducer devices with a large hole diameter for producing microbubbles, as oxygenation source. This innovation provides a new approach to the aeration systems for use in simple aquaculture installations. The results showed that the MBG DIYM $O_2^{RS}$, using a large diameter nozzle, draws air from large holes to overcome obstacles due to blockage.

**Acknowledgements**. The authors would like to thank to the Technical Team, who provided research facilities at ITP Punaga and to Dr. A. Indra Jaya Asaad, S.Pi, MSc, the head of Research Institute For Coastal Aquaculture And Fisheries Extention, for the full support to this study. This study is part of the Hasanuddin University PhD research study supported by DIPA BRPBAP3 (032.12.2.403828/2019).

**Conflict of interest**. The authors declare no conflict of interest.

## References

Abbas G., Zheng P., Wang L., Li W., Zhang M., Zhang J., 2014 Oxygen transfer characteristics in a pilot-scale airlift internal-loop bioreactor for simultaneous partial nitrification and anaerobic ammonia oxidation. Environmental Engineering Science 31(8):453–460.

Abdelrahman H. A., Veverica K. L., 2016 Testing micro-nanobubble generating device at different salinities. The Global Aquaculture Advocate, pp. 7–12.

Adel M., Shaalan M. R., Kamal R. M., Monayeri D. S. E., 2019 A comparative study of impeller aerators configurations. Alexandria Engineering Journal 58(4):1431-1438.

Ahmad T., 1987 Evaluation of wheel aerator design for use in fish culture ponds. Aurburn University, 85 p.
Alam H. S., Redhyka G. G., Bahrudin, Sugiarto A. T., Salim T. I., Mardhiya I. R., 2018 Design and performance of swirl flow microbubble generator. International Journal of Engineering and Technology (UAE) 7(4):66–69.
Allan G. L., Maguire G. B., 1991 Lethal levels of low dissolved oxygen and effects of short-term oxygen stress on subsequent growth of juvenile *Penaeus monodon*. Aquaculture 94(1):27–37.
Basso A., Hamad F. A., Ganesan P., 2018 Effects of the geometrical configuration of air–water mixer on the size and distribution of microbubbles in aeration systems. Asia-Pacific Journal of Chemical Engineering 13(6):1–11.
Boyd C. E., 1986 A method for testing aerators for fish tanks. Progressive Fish-Culturist 48:68–70.
Boyd C. E., 1989 Water quality management and aeration in shrimp farming. Fisheries and Allied Aquacultures Departmental Series No. 2, 84 p.
Boyd C. E., 1998 Pond water aeration systems. Aquacultural Engineering 18(1):9–40.
Boyd C. E., Ahmad T., 1987 Evaluation of aerators for channel catfish farming. Alabama Agricultural Experiment Station Auburn University Lowell T Frobish Bulletin 52:1-52.
Boyd C. E., Tucker C. S., 1998 Pond aquaculture water quality management. Kluwer Academic Publishers, 711 p.
Boyd C. E., Tucker C. S., 2014 Handbook for aquaculture water quality. C. E. Boyd & Associates Incorporated, 439 p.
Budhijanto W., Darlianto D., Pradana Y. S., Hartono M., 2017 Application of micro bubble generator as low cost and high efficient aerator for sustainable fresh water fish farming. International Seminar on Fundamental and Application of Chemical Engineering 1840(110008):1-8.
Cubas J. M. C., Stel H., Ofuchi E. M., Neto M. A. M., Morales R. E. M., 2020 Visualization of two-phase gas-liquid flow in a radial centrifugal pump with a vaned diffuser. Journal of Petroleum Science and Engineering 187(106848):1-14.
Dai C., Guo J., Liu J., Dong L., Liu H., 2020 Experimental study on aeration performance and bubble characteristics of inverted umbrella aerator. Water 12(10):1–5.
Eckenfelder W. W., Malina J. F., Patterson J. W., 2002 Aeration: Principles and practice. CRC Press, 349 p.
Heriyati E., Rustadi R., Isnansetyo A., Triyatmo B., 2020 [Microbubble aeration test in determining water quality, Nutrition Value Coefficient (NVC), Condition Factor (K) and aquaculture performance red tilapia (*Oreocrhomis* sp.)]. Jurnal Pertanian Terpadu 8(1):27–41. [In Indonesian].
Herrmann-Heber R., Reinecke S. F., Hampel U., 2020 Dynamic aeration for improved oxygen mass transfer in the wastewater treatment process. Chemical Engineering Journal 386(122068):1–9.
Huang J., Sun L., Du M., Liang Z., Mo Z., 2019 An investigation on the performance of a micro-scale Venturi bubble generator. Chemical Engineering Journal 386(120980):1–12.
Huang J., Sun L., Liu H., Mo Z., Tang J., Xie G., Du M., 2020 A review on bubble generation and transportation in Venturi-type bubble generators. Experimental and Computational Multiphase Flow 2(3):123–134.
Itoh K., Kashino Y., Ifuku K., Kouji M., Yamamoto T., Taguchi S., 2019 Dispersed air flotation of microalgae using venturi tube type microbubble generator. Biomass and Bioenergy 130(105379):1–5.
Jayanthi M., Balasubramaniam A. A. K., Suryaprakash S., Veerapandian N., Ravisankar T., Vijayan K., 2021 Aquacultural engineering assessment of standard aeration efficiency of different aerators and its relation to the overall economics in shrimp culture. Aquacultural Engineering 92(102142):1–10.
Jayraj P., Roy S. M., Mukherjee C. K., Mal B. C., 2018 Design characteristics of submersible aerator. Turkish Journal of Fisheries and Aquatic Sciences 18:1017–1023.

Jeon S.-Y., Yoon J.-Y. Y., Jang C.-M. M., 2018 Bubble size and bubble concentration of a microbubble pump with respect to operating conditions. Energies 11(7):1–13.
Juwana W. E., Widyatama A., Dinaryanto O., Budhijanto W., Indarto, Deendarlianto, 2019 Hydrodynamic characteristics of the microbubble dissolution in liquid using orifice type microbubble generator. Chemical Engineering Research and Design 141:436–448.
Lee C. H., Choi H., Jerng D. W., Kim D. E., Wongwises S., Ahn H. S., 2019 Experimental investigation of microbubble generation in the venturi nozzle. International Journal of Heat and Mass Transfer 136:1127–1138.
Majid A. I., Nugroho F. M., Juwana W. E., Budhijanto W., Deendarlianto, Indarto, 2018 On the performance of venturi-porous pipe microbubble generator with inlet angle of 20° and outlet angle of 12°. Proceedings of the 9th International Conference on Thermofluids 2001(050009):1-10.
Marappan J., Anathaikamatchi B. A., Sakkarai S., Thiagarajan R., Muthusamy D., Kuppusamy M., Shanmugam S., 2020 Assessment of the new generation aeration systems efficiency and water current flow rate, its relation to the cost economics at varying salinities for *Penaeus vannamei* culture. Aquaculture Research 51(5):2112–2124.
Masakazu K., Haruaki K., Yoshiaki I., Jun T., Toshihiro F., Koichi T., 2011 Development of high density nano-bubbles generation system by nanoGALF technology. Japanese Society for Multiphase Flow, pp. 2–3.
Mukherjee S. C., Chandrakant M. H. E., 2003 Course manual. Aquaculture Engineering. Central Institute of Fisheries Education, 291 p.
Ruttanagosrigit W., Musig Y., Boyd C. E., Sukchareon L., 1991 Effect of salinity on oxygen transfer by propeller-aspirator-pump and paddle wheel aerators used in shrimp farming. Aquacultural Engineering 10(2):121–131.
Sadatomi M., Kawahara A., Kano K., Ohtomo A., 2005 Performance of a new micro-bubble generator with a spherical body in a flowing water tube. Experimental Thermal and Fluid Science 29(5):615–623.
Sadatomi M., Kawahara A., Matsuura H., Shikatani S., 2012 Micro-bubble generation rate and bubble dissolution rate into water by a simple multi-fluid mixer with orifice and porous tube. Experimental Thermal and Fluid Science 41:23–30.
Stenstrom M. K., Gilbert R. G., 1981 Effects of alpha, beta and theta factor upon the design, specification and operation of aeration systems. Water Research 15(6): 643–654.
Tierney T. W., Fleckenstein L. J., Ray A. J., 2020 The effects of density and artificial substrate on intensive shrimp *Litopenaeus vannamei* nursery production. Aquacultural Engineering 89(102063):1–5.
Tsutsumi H., 2010 Application of microbubble injector to marine fish farming and its future perspective. Bulletin of the Society of Sea Water Science Japan 64:31–38.
Wang X., Shuai Y., Zhang H., Sun J., Yang Y. Y., Huang Z., Jiang B., Liao Z., Wang J., Yang Y. Y., 2020 Bubble breakup in a swirl-venturi microbubble generator. Chemical Engineering Journal 403(126397):1–11.
Warjito, Taukhid I., Pamungkas A., Adiyana K., Setyantono M., 2016 [Skimmer protein characterization]. Seminar Nasional Teknologi dan Rekayasa (SENTRA), pp. 1–8. [In Indoensian].
Wilson D. A. D. A., Pun K., Ganesan P. B. P. B., Hamad F., 2021 Geometrical optimization of a venturi-type microbubble generator using CFD simulation and experimental measurements. Designs 5(1):1–18.
Zhang C., Song B., Shan J., Ni Q., Wu F., Wang S., 2020 Design and optimization of a new tube aeration device. Aquaculture International 28(3):985–999.
*** ASCE, 2007 Measurement of oxygen transfer in clean water. American Society of Civil Engineers.

Received: 01 June 2021. Accepted: 13 August 2021. Published online: 30 August 2021.
Authors:
Imam Taukhid, PhD Student Fisheries Science, Faculty of Marine Science And Fisheries, Hasanuddin University, Jl. Perintis Kemerdekaan KM. 10, Makassar, 90245 South Sulawesi, Indonesia, e-mail: imam_t@kkp.go.id
Dody Dharmawan Trijuno, Department of Aquaculture, Faculty of Marine Science and Fishery, Hasanuddin University, Jl. Perintis Kemerdekaan KM. 10, Makassar, 90245 South Sulawesi, Indonesia, e-mail: dodytrijuno@gmail.com
Muhammad Yusri Karim, Department of Aquaculture, Faculty of Marine Science and Fishery, Hasanuddin University, Jl. Perintis Kemerdekaan KM. 10, Makassar, 90245 South Sulawesi, Indonesia, e-mail: yusri_karim@yahoo.com
Rachman Syah, Ministry of Marine Affairs and Fisheries Research Institute for Coastal Aquaculture and Fisheries Extention, 90512 Maros, Indonesia, e-mail: rachman222000@yahoo.com
Makmur, Ministry of Marine Affairs and Fisheries Research Institute for Coastal Aquaculture and Fisheries Extention, 90512 Maros, Indonesia, e-mail: fauzanmakmur17@yahoo.co.id

How to cite this article:
Taukhid I., Trijuno D. D., Karim M. Y., Syah R., Makmur, 2021 Performance of a novel aeration microbubble generator in aquaculture. AACL Bioflux 14(4):2478-2486.